Sharp Lines Due to Cr3+ and Mn2+ Impurities in Insulators: Going Beyond the Usual Tanabe–Sugano Approach

ARTICLE *in* THE JOURNAL OF PHYSICAL CHEMISTRY A · FEBRUARY 2014

Impact Factor: 2.69 · DOI: 10.1021/jp5010067 · Source: PubMed

5 AUTHORS, INCLUDING:

Miguel Moreno
Universidad de Cantabria
224 PUBLICATIONS **2,712** CITATIONS

SEE PROFILE

THE JOURNAL OF PHYSICAL CHEMISTRY A

Article

pubs.acs.org/JPCA

Sharp Lines Due to Cr^{3+} and Mn^{2+} Impurities in Insulators: Going Beyond the Usual Tanabe−Sugano Approach

J. M. García-Lastra,*[,†,‡] P. García-Fernández,[§] M. T. Barriuso,[∥] J. A. Aramburu,[§] and M. Moreno[§]

[†]Center for Atomic-scale Materials Design, Department of Physics, Technical University of Denmark, DK-2800 Kongens Lyngby, Denmark

[‡]Deparment of Energy Conversion and Storage, Technical University of Denmark, DK-4000 Roskilde, Denmark

[§]Departamento de Ciencias de la Tierra y Física de la Materia Condensada, Universidad de Cantabria, Avenida de los Castros s/n, 39005 Santander, Spain

[∥]Departamento de Física Moderna, Universidad de Cantabria, Avenida de los Castros s/n, 39005 Santander, Spain

ABSTRACT: This work is aimed at understanding the different behavior of optical sharp lines (corresponding to 10Dq-independent transitions) of Mn^{2+} and Cr^{3+} in normal and inverted perovskites that cannot be explained within the usual Tanabe-Sugano approach. In particular, we want to clarify why on passing from $KMgF_3$:M to $LiBaF_3$:M (M = Mn^{2+}, Cr^{3+}) the energy, $E(^6A_1 \rightarrow {}^4A_1)$, for Mn^{2+} decreases by $\Delta = 1100\ cm^{-1}$, while $\Delta < 100\ cm^{-1}$ for the energy $E(^2E \rightarrow {}^4A_2)$ corresponding to Cr^{3+}. The origin of this surprising difference in these model systems is clarified by writing the transition energies of MF_6 complexes through the ten Coulomb and exchange integrals consistent with the cubic symmetry and not considered in the usual Tanabe−Sugano approach. It is shown that $E(^6A_1 \rightarrow {}^4A_1)$ depends on exchange integrals $K(3z^2 - r^2, xy)$ and $K(x^2 - y^2, xy)$, while $E(^2E \rightarrow {}^4A_2)$ depends on $K(xz, yz)$ where the two involved electrons display a π character. These exchange integrals have been calculated just considering a MF_6 unit subject to the internal electric field due to the rest of the lattice ions. In addition to a reasonably reproduction of the main trends observed experimentally for the model systems, the present calculations prove that the exchange integrals are not related in a simple way to the covalency of involved orbitals. Particular attention is also paid to explain why the transitions, which are 10Dq-independent are less sensitive to the host lattice change than those which do depend on 10Dq. The present work shows that $K(xz, yz)$ for Cr^{3+} is particularly insensitive to the host lattice change and thus sheds light on the origin of the near independence of $E(^2E \rightarrow {}^4A_2)$ along the series of oxides doped with such an impurity .

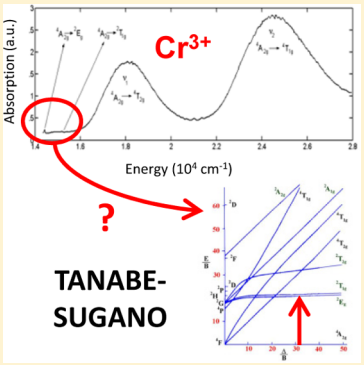

1. INTRODUCTION

Transition metal (TM) ions in insulating materials have excitations in the optical range due to the multiplets emerging from the d^n configuration ($0 < n < 10$) of the d ion. Although these excitations reflect the chemical bonding between the impurity, M, and the ligands, X, of the MX_N complex, where active electrons are essentially confined, not all of them display the same sensitivity to host lattice changes or hydrostatic pressures. Indeed, for cubic or nearly cubic MX_N complexes, such changes are much less felt by transitions whose energy, E, is independent of the cubic field splitting parameter, 10Dq, than in the opposite case.[1−3] Accordingly, 10Dq-independent transitions give rise to sharp lines whose inhomogeneous bandwidth (∼1−10 cm^{-1}) is caused by random strains,[1,4] while for transitions which do depend on 10Dq, the associated band is usually much broader with a bandwidth on the order of 2000 cm^{-1}. The origin of the strong dependence of 10Dq to changes of the metal−ligand distance, R, is discussed in refs 5 and 6.

A 10Dq-independent transition which has widely been studied is the sharp $^2E \rightarrow {}^4A_2$ emission line observed for Cr^{3+}-doped oxides.[7−9] As shown in Table 1, the energy, $E(^2E \rightarrow {}^4A_2)$, of such a transition varies less than 1.8% for a series of Cr^{3+}-doped oxides, while the corresponding changes of 10Dq are around 15%. Similarly (Table 2), the value of the energy of sharp line $E(^2E \rightarrow {}^4A_2)$ for $LiBaF_3:Cr^{3+}$ is identical to that observed for $KMgF_3:Cr^{3+}$ within 0.5%, although 10Dq is 11% higher for the former system.[10,11] Due to both facts, $LiBaF_3$ is the only fluoride where the Cr^{3+} emission at $T = 20$ K and ambient pressure comes from the ^2E state[10] and not from the $^4T_2$ one, such as is observed for $KMgF_3:Cr^{3+}$[11] and other doped fluorides, like $KZnF_3:Cr^{3+}$,[12] $K_2NaNF_6:Cr^{3+}$ (N = Ga and Sc),[13,14] $Rb_2KGaF_6:Cr^{3+}$,[15] or $Cs_2NaNF_6:Cr^{3+}$ (N = Y and Al).[16,17] Nevertheless, in cases[11,12] like $KMgF_3:Cr^{3+}$ or

Table 1. Experimental Energies (in cm^{-1}) of $^4A_2 \rightarrow {}^4T_2$ and $^2E \rightarrow {}^4A_2$ Transitions Corresponding to Several Doped Oxides Containing CrO_6^{9-} Units

	ruby	emerald	$Mg_2AlO_4:Cr^{3+}$
$^4A_2 \rightarrow {}^4T_2$	18070	16130	18520
$^2E \rightarrow {}^4A_2$	14420	14690	14600
reference	7 and 8	7 and 8	8 and 9

Received: February 26, 2014
Published: February 28, 2014

   dx.doi.org/10.1021/jp5010067 | J. Phys. Chem. A 2014, 118, 2377−2384

Table 2. Experimental Values of $E(^2E \rightarrow {}^4A_2)$ and 10Dq Energies for Cr^{3+}-doped $KMgF_3$ and $LiBaF_3$ Cubic Lattices Together with the Values of $E(^6A_1 \rightarrow {}^4A_1)$ and 10Dq Energies for the Mn^{2+} Impurity in the Same Lattices[a]

impurity	transition energy	$KMgF_3$	$LiBaF_3$	ref
Cr^{3+}	$E(^2E \rightarrow {}^4A_2)$	15100	15030	10 and 11
	10Dq	15150	16720	
Mn^{2+}	$E(^6A_1 \rightarrow {}^4A_1)$	25200	24096	3 and 19
	10Dq	8430	9795	

[a]All energies are given in cm^{-1} units.

$KZnF_3:Cr^{3+}$, the sharp $^2E \rightarrow {}^4A_2$ emission line becomes observable under hydrostatic pressure.

A somewhat different situation is found when comparing the results for the Mn^{2+} impurity in $KMgF_3$ (normal perovskite structure)[3] and in the inverted perovskite $LiBaF_3$,[18,19] where in both *cubic* lattices (Figure 1) an octahedral MnF_6^{4-} complex

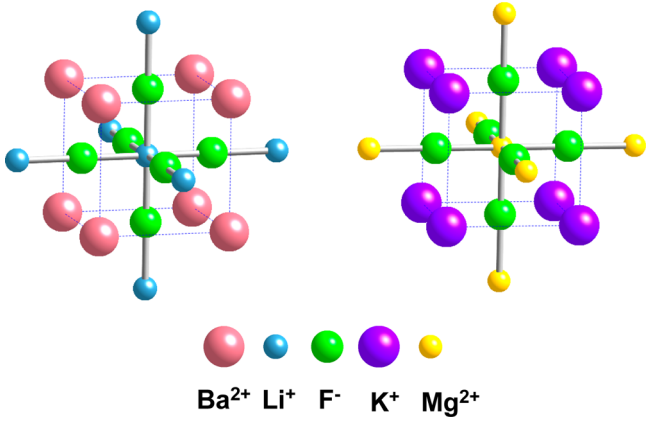

Figure 1. Unit cells (marked with dashed lines) of the inverse $BaLiF_3$ (left) and normal $KMgF_3$ (right) perovskite structures. The central ion (Li^+ in $BaLiF_3$ and Mg^{2+} in $KMgF_3$) is replaced by Mn^{2+} and Cr^{3+} in the calculations. The second neighbors in [100], [010], and [001] directions are also shown.

can be formed (Table 2). Although in $LiBaF_3:Mn^{2+}$, the impurities enter the Li^+ sites, cubic centers with remote charge compensation are formed such as it happens for $MgO:Cr^{3+}$[20] or $KMgF_3:A^{3+}$ (A = Cr and Fe).[11,21] While the experimental 10Dq value increases by 16% on passing from $KMgF_3:Mn^{2+}$[3] to $LiBaF_3:Mn^{2+}$,[19] there are also significant changes in the energy of the sharp $^6A_1 \rightarrow {}^4A_1$ transition despite it being fully 10Dq-independent. As is shown in Table 2, the transition energy $E(^6A_1 \rightarrow {}^4A_1)$ experiences a decrease, Δ, of 1100 cm^{-1} (4.4%) when $KMgF_3$ is replaced by $LiBaF_3$ as host lattice, while the value $E(^6A_1 \rightarrow {}^4A_1) = 25200$ cm^{-1} is practically the same for cubic fluoroperovskites (like $CsCaF_3$ or $KMgF_3$) doped with Mn^{2+}.[3] Thus the Δ = 1100 cm^{-1} decrease of $E(^6A_1 \rightarrow {}^4A_1)$ on going from $KMgF_3:Mn^{2+}$[3] to $LiBaF_3:Mn^{2+}$[19] is surprisingly much bigger than that experienced by $E(^2E \rightarrow {}^4A_2)$, corresponding to the Cr^{3+} impurity.

With these facts in mind, this work is addressed to clarify, by means of ab initio calculations, why the sharp $^6A_1 \rightarrow {}^4A_1$ transition of MnF_6^{4-} is more sensitive to the replacement of $KMgF_3$ by $LiBaF_3$ as host lattice than the $^2E \rightarrow {}^4A_2$ transition of CrF_6^{3-}, despite both being 10Dq-independent. Due to the cubic symmetry of both host lattices, $KMgF_3:M$ and $LiBaF_3:M$ (M = Mn^{2+}, Cr^{3+}) can be considered *model systems* for exploring the influence of the host lattice upon the multiplets of TM impurities.

As for TM impurities in insulators, active electrons are essentially *localized* in the MX_N complex, the electronic properties due to the impurity can be explained merely considering that complex but taking into account the action of the electrostatic potential coming from the rest of the lattice ions, $V_R(\mathbf{r})$.[22] This electrostatic potential, seen by the electrons *confined* in the complex, has been shown to be the responsible for the different colors displayed by the ruby, emerald, and alexandrite[22−24] and also for the higher 10Dq value for $LiBaF_3:M$ when compared to that for $KMgF_3:M$ (M = Ni^{2+}, Co^{2+}, Mn^{2+}, and Cr^{3+}).[25] Therefore, it is challenging to explore the origin of the different sensitivity of $E(^6A_1 \rightarrow {}^4A_1)$ and $E(^2E \rightarrow {}^4A_2)$ excitation energies to the host lattice change using the same procedure.

It should be noted now that the multiplets of a d^n impurity in a cubic insulator are *not properly described* by the two *B* and *C* Racah parameters and 10Dq,[26] such as is done in the usual Tanabe−Sugano procedure.[26,27] Indeed, even if, as a first approximation, we consider the configuration mixing only within the d^n configuration, there are ten, and not two, independent parameters (involving Coulomb and exchange integrals) as a result of the O_h symmetry.[27,28] The reduction of ten to only two parameters is made *assuming* that, for calculating the multiplets, the wave function, $|\phi_i\rangle$, of an antibonding e_g or t_{2g} orbital can simply be taken as[27,28]

$$|\phi_i\rangle = \eta|d_i\rangle \tag{1}$$

where $|d_i\rangle$ is a pure *d*-wavefunction and the covalency parameter $\eta \leq 1$ has the same value for both e_g or t_{2g} orbitals. This assumption is in general not right, as for octahedral complexes, electron paramagnetic resonance (EPR) data, and theoretical calculations[5,6,18,22,26−29] support that $\eta^2(e_g) < \eta^2(t_{2g})$. Due to this approximation, it is not surprising that some experimental results cannot be understood within the simple Tanabe−Sugano procedure, despite being widely used for *fitting* the measured peaks observed in optical spectra. For instance, from the experimental $E(^2E \rightarrow {}^4A_2)$ values for Cr^{3+}-doped oxides (Table 1), it seems that Racah parameters are practically the same along the series while a different conclusion is reached looking at the energy difference of $^4A_2 \rightarrow {}^4T_1$ and $^4A_2 \rightarrow {}^4T_2$ transitions, $\Delta(^4T_1; {}^4T_2)$, such as it is pointed out in ref 26.

Seeking to gain a better insight into the present problem, we have tried as a first step to write the expressions of $E(^6A_1 \rightarrow {}^4A_1)$ and $E(^2E \rightarrow {}^4A_2)$ transition energies working only within the d^n configuration ($n = 3$ for Cr^{3+} and $n = 5$ for Mn^{2+}) in terms of the ten independent parameters. Thus, in the present approach, the interaction with other electronic configurations is not considered, but we expect to reproduce the *main trends* observed on passing from $KMgF_3:M$ to $LiBaF_3:M$ (M = Mn^{2+} and Cr^{3+}). In a second step, we want to calculate the values of $E(^6A_1 \rightarrow {}^4A_1)$ and $E(^2E \rightarrow {}^4A_2)$ within the present approximation as well as the values of the involved parameters. Particular attention is paid to explore whether the changes in $E(^6A_1 \rightarrow {}^4A_1)$ and $E(^2E \rightarrow {}^4A_2)$ due to the replacement of $KMgF_3$ by $LiBaF_3$ can be understood *only* in terms of variations of the electronic charge on the central cation.[30]

This work is arranged as follows. In Section 2, the expressions of $E(^6A_1 \rightarrow {}^4A_1)$ and $E(^2E \rightarrow {}^4A_2)$ transition energies for an octahedral MX_6 complex in terms of the ten

dx.doi.org/10.1021/jp5010067 | J. Phys. Chem. A 2014, 118, 2377−2384

independent integrals are reported. In Section 3, a short account of employed computational methods is provided, while main results of this work are given in Section 4. Some final remarks are displayed in the last section.

2. EXPRESSIONS OF $E(^6A_1 \rightarrow {}^4A_1)$ AND $E(^2E \rightarrow {}^4A_2)$ ENERGIES

For an octahedral Cr^{3+} complex, both the ground state, $^4A_2$, and the ^2E excited state essentially arise from the t_{2g}^3 configuration.[1,2,26,27] For clearing up the notation, we call $t_{2g}(xy)$ to the antibonding molecular orbital of the MX_6 complex transforming like xy. The expression of $E(^2E \rightarrow {}^4A_2)$ for an octahedral Cr^{3+} complex in the strong field approximation is given in ref 27 and it is equal to

$$E(^2E \rightarrow {}^4A_2) = 3K(xz, yz) \tag{2}$$

Here $K(xz, yz) = K(xy, xz) = K(xy, yz)$ is an exchange integral involving two different t_{2g} orbitals exhibiting a π character under octahedral symmetry. As shown in refs 27 and 28, $E(^2E \rightarrow {}^4A_2)$ is practically independent of 10Dq when 10Dq > 8000 cm^{-1}, thus pointing out that the configuration interaction of the first excited state ^2E with higher ones of the same label plays a minor role. Experimental 10Dq values for Cr^{3+} in fluorides and oxides under octahedral coordination are typically lying in the range from 15000 to 19000 cm^{-1}.[7−9,13−17]

As for the expression of $E(^6A_1 \rightarrow {}^4A_1)$ for an octahedral Mn^{2+} complex in terms of the ten independent Coulomb and exchange integrals, not directly given in ref 27, it can routinely be calculated. For doing so, the ground state wave function $|^6A_1; M = 5/2\rangle$ is just described by means of a single Slater determinant

$$|^6A_1; M = 5/2\rangle = |xy, \alpha; xz, \alpha; yz, \alpha; 3z^2 - r^2, \alpha; x^2 - y^2, \alpha| \tag{3}$$

It is worth noting now that considering only the 252 states emerging from the d^5 configuration there is *only one* $^4A_1$ state, a matter which simplifies its description with respect to most of the states where the configuration interaction cannot be avoided.

Due to symmetry reasons, the wave function $|^4A_1; M = 3/2\rangle$ of the $^4A_1$ excited state can be written as

$$\begin{aligned}|^4A_1; M = 3/2\rangle = a\{&|xy, \beta; xz, \alpha; yz, \alpha; 3z^2 - r^2, \alpha; x^2 - y^2, \alpha| \\ &+ |xy, \alpha; xz, \beta; yz, \alpha; 3z^2 - r^2, \alpha; x^2 - y^2, \alpha| \\ &+ |xy, \alpha; xz, \alpha; yz, \beta; 3z^2 - r^2, \alpha; x^2 - y^2, \alpha|\} \\ + b&|xy, \alpha; xz, \alpha; yz, \alpha; 3z^2 - r^2, \beta; x^2 - y^2, \alpha| \\ + c&|xy, \alpha; xz, \alpha; yz, \alpha; 3z^2 - r^2, \alpha; x^2 - y^2, \beta|\end{aligned} \tag{4}$$

Bearing in mind that

$$\begin{aligned}S^2|^4A_1; M = 3/2\rangle &= (15/4)|^4A_1; M = 3/2\rangle \\ S_Z|^4A_1; M = 3/2\rangle &= (3/2)|^4A_1; M = 3/2\rangle\end{aligned} \tag{5}$$

a normalized $|^4A_1; M = 3/2\rangle$ wave function requires that $a = -2/\sqrt{30}$ and $b = c = 3/\sqrt{30}$, in agreement with ref 31. Using now the general procedure described in ref 27, the value of the $E(^6A_1 \rightarrow {}^4A_1)$ energy transition can be expressed in terms of independent Coulomb and exchange integrals as follows

$$E(^6A_1 \rightarrow {}^4A_1) = (5/2)\{K(3z^2 - r^2, xy) + K(x^2 - y^2, xy)\} \tag{6}$$

This expression is thus relatively simple because in the description of $^4A_1$, the configuration interaction with other states within the d^5 manifold is not allowed and thus $E(^6A_1 \rightarrow {}^4A_1)$ only depends on two among the ten independent parameters. If we now assume that the involved one-electron wave functions are purely d-wavefunctions multiplied by a constant, such as was described in eq 1, then $K(3z^2 - r^2, xy) = 4B + C$ and $K(3z^2 - r^2, xy) = C$, and thus under such an approximation it is found that $E(^6A_1 \rightarrow {}^4A_1) = 10B + 5C$, in agreement with well-known results.[27,28]

If we compare this result with $E(^2E \rightarrow {}^4A_2) = 9B + 3C$, derived under the same approximation for d^3 complexes,[27] it is certainly not easy to understand why the $E(^6A_1 \rightarrow {}^4A_1)$ energy of Mn^{2+} impurity is more sensitive than $E(^2E \rightarrow {}^4A_2)$ of Cr^{3+} to the replacement of $KMgF_3$ by $LiBaF_3$ as the host lattice. A different situation holds, however, within the ten parameters framework consistent with the cubic symmetry of complexes. Indeed, eq 6 points out that $E(^6A_1 \rightarrow {}^4A_1)$ depends on the exchange between a π electron of the t_{2g} orbital and another σ electron of the e_g orbital. Therefore, at this level of the theory, there is already a qualitative difference with $E(^2E \rightarrow {}^4A_2)$, driven by an exchange integral involving two π electrons, as shown in eq 2.

3. COMPUTATIONAL DETAILS

First-principles calculations were performed within the frameworks of the density functional theory (DFT) and Hartree−Fock theory (HF) by means of the Amsterdam density functional (ADF) code,[32] version 2012.01. In order to be sure about the reliability of main trends, calculations have been carried out using four levels of approximation for the exchange-correlation potential; namely (i) local density approximation (LDA), employing the Vosko−Wilk−Nusair (VWN) functional,[33] (ii) general gradient approximation (GGA) using the Becke−Perdew (BP) functional,[34,35] (iii) a hybrid scheme mixing GGA and exact HF exchange with the so-called PBE0 functional,[36] and (iv) a pure HF calculation. Atoms were described through TZP quality basis sets (triple-ζ Slater type orbitals plus one polarization extra function) for the metal and DZP (double-ζ Slater type orbitals plus one polarization extra function) for the ligands, keeping core electrons frozen (1s-3p for Cr and Mn and 1s for F). All the calculations performed in the present work were spin-unrestricted. We checked that the influence of the spin contamination on the results was negligible.

In order to evaluate the exchange integrals, we used 7 ions clusters, MF_6^{q-} (q = 3 for M = Cr and q = 4 for M = Mn), embedded in an electrostatic potential from the rest of lattice ions, $V_R(\mathbf{r})$. The $V_R(\mathbf{r})$ potential was simulated by means of a set of point charges (about 250), located in lattice positions around the cluster, whose charge value itself was fitted in order to reproduce the potential inside the cluster due to the infinite lattice by use of an Evjen−Ewald scheme.[37] The equilibrium metal−ligand distance, R_0, was fixed at the values found in references 25 and 26 [R_0(Cr−F) = 1.900 Å and R_0(Mn−F) = 2.065 Å], which are the same for both $KMgF_3$ and $LiBaF_3$ host

dx.doi.org/10.1021/jp5010067 | J. Phys. Chem. A 2014, 118, 2377−2384

lattices due to the nearly identical ionic radii of Mg^{2+} and Li^{+} ions.

For obtaining the exchange integrals involved in eqs 2 and 6, we have first calculated the energy of several Slater determinants through a full self-consistent field (SCF) procedure (i.e., we have calculated the total energies of the Slater determinants using their particular d-orbital occupations). Once the energy of these Slater determinants is known, the exchange integrals can simply be written as a linear combination of them. This strategy is similar to that proposed by Atanasov et al.[38,39] in their ligand field-DFT (LF-DFT) scheme, but with two main differences: (i) in LF-DFT, the energy of the Slater determinants is computed using the wave functions from an "average of occupations" calculation in which d electrons are equally split in the 10 d orbitals. After freezing the wave functions, the occupation number of d-orbitals is set for each Slater-determinant, and the energies are obtained through a post-SCF calculation. By contrast, in our approximation, the wave functions are not kept frozen when calculating the energy of different Slater determinants. (ii) In LF-DFT the energy of all possible Slater determinants is calculated and then the exchange (and direct) integrals are obtained by solving the overdetermined system of linear equations. The overdetermined system is used because in DFT, due to its problems with the symmetry in the exchange term, the energy of the integrals depends on the particular set of Slater determinants chosen to calculate it. However, in HF theory, the symmetry properties of the exchange term are kept and, in principle, the energy of the integrals should not depend on the particular choice of Slater integrals. For this reason in our approach, we have used only a few Slater determinants (the minimum amount to be able to obtain the integrals) within HF theory. Later on, we performed DFT calculations using the same choice of Slater determinants, checking that the trends explored in this work are the same with HF and DFT calculations.

For calculating the exchange integrals $K(xz, yz)$, $K(xy, x^2 - y^2)$, and $K(xy, 3z^2 - r^2)$ in the case of CrF_6^{3-}, a possible choice of Slater determinants is the following

$$
\begin{aligned}
2K(x^2 - y^2, xy) &= -E\{|xy, \alpha; 3z^2 - r^2, \alpha; x^2 - y^2, \alpha|\} \\
&\quad - E\{|xy, \alpha; 3z^2 - r^2, \alpha; x^2 - y^2, \beta|\} \\
&\quad + E\{|xy, \alpha; 3z^2 - r^2, \beta; x^2 - y^2, \alpha|\} \\
&\quad + E\{|xy, \alpha; 3z^2 - r^2, \beta; x^2 - y^2, \beta|\} \\
2K(3z^2 - r^2, xy) &= -E\{|xy, \alpha; 3z^2 - r^2, \alpha; x^2 - y^2, \alpha|\} \\
&\quad + E\{|xy, \alpha; 3z^2 - r^2, \alpha; x^2 - y^2, \beta|\} \\
&\quad + E\{|xy, \alpha; 3z^2 - r^2, \beta; x^2 - y^2, \alpha|\} \\
&\quad - E\{|xy, \alpha; 3z^2 - r^2, \beta; x^2 - y^2, \beta|\} \\
2K(xz, yz) &= E\{|xy, \alpha; xz, \alpha; yz, \beta|\} \\
&\quad - E\{|xy, \alpha; xz, \alpha; yz, \alpha|\}
\end{aligned}
\tag{7}
$$

This choice has been motivated by the significant dependence of these five Slater determinants on the exchange integrals. Bearing in mind that the Slater determinants should belong to A_1, when necessary we have performed the calculations under a very small D_{2h} distortion where ligands are moved less than 0.1 pm with respect to the perfect octahedral geometry.

A similar procedure has been employed for deriving the three $K(xz, yz)$, $K(xy, x^2 - y^2)$, and $K(xy, 3z^2 - r^2)$ integrals for the MnF_6^{4-} complex. In this case, the choice of Slater determinants is given by

$$
\begin{aligned}
2K(x^2 - y^2, xy) &= E\{|xy, \alpha; xz, \alpha; yz, \alpha; 3z^2 \\
&\quad - r^2, \alpha; x^2 - y^2, \alpha|\} \\
&\quad + E\{|xy, \beta; xz, \alpha; yz, \alpha; 3z^2 - r^2, \alpha; x^2 - y^2, \beta|\} \\
&\quad - E\{|xy, \alpha; xz, \alpha; yz, \alpha; 3z^2 - r^2, \alpha; x^2 - y^2, \beta|\} \\
&\quad - E\{|xy, \beta; xz, \alpha; yz, \alpha; 3z^2 - r^2, \alpha; x^2 - y^2, \alpha|\} \\
2K(3z^2 - r^2, xy) &= E\{|xy, \alpha; xz, \alpha; yz, \alpha; 3z^2 \\
&\quad - r^2, \alpha; x^2 - y^2, \alpha|\} \\
&\quad + E\{|xy, \beta; xz, \alpha; yz, \alpha; 3z^2 - r^2, \beta; x^2 - y^2, \alpha|\} \\
&\quad - E\{|xy, \alpha; xz, \alpha; yz, \alpha; 3z^2 - r^2, \beta; x^2 - y^2, \alpha|\} \\
&\quad - E\{|xy, \beta; xz, \alpha; yz, \alpha; 3z^2 - r^2, \alpha; x^2 - y^2, \alpha|\} \\
2K(xz, yz) &= E\{|xy, \alpha; xz, \alpha; yz, \alpha; 3z^2 - r^2, \alpha; x^2 \\
&\quad - y^2, \alpha|\} + E\{|xy, \alpha; xz, \alpha; yz, \alpha; 3z^2 - r^2, \beta; x^2 \\
&\quad - y^2, \beta|\} - E\{|xy, \beta; xz, \alpha; yz, \alpha; 3z^2 - r^2, \alpha; x^2 \\
&\quad - y^2, \alpha|\} - E\{|xy, \beta; xz, \alpha; yz, \alpha; 3z^2 - r^2, \beta; x^2 \\
&\quad - y^2, \beta|\}
\end{aligned}
\tag{8}
$$

4. RESULTS AND DISCUSSION

Let us now discuss the values of $E(^6A_1 \rightarrow {}^4A_1)$ and $E(^2E \rightarrow {}^4A_2)$ transition energies derived by means of eqs 2, 6, 7, and 8 within the d^n configuration ($n = 5$ for Mn^{2+} and $n = 3$ for Cr^{3+}).

Values of $E(^6A_1 \rightarrow {}^4A_1)$ energies for both $KMgF_3$:Mn^{2+} and $LiBaF_3$:Mn^{2+} centers calculated using the VWN, BP, and PBE0 functionals, and also within the HF framework, are reported in Table 3 together with the corresponding experimental values.

Table 3. Calculated Values of $E(^6A_1 \rightarrow {}^4A_1)$ and $E(^2E \rightarrow {}^4A_2)$ Transition Energies for Mn^{2+} and Cr^{3+} Impurities in both $KMgF_3$ and $LiBaF_3$ Host Lattices by Means of Four Different Approaches[a]

	$E(^6A_1 \rightarrow {}^4A_1)$		$E(^2E \rightarrow {}^4A_2)$	
functional	$KMgF_3$:Mn^{2+}	$LiBaF_3$:Mn^{2+}	$KMgF_3$:Cr^{3+}	$LiBaF_3$:Cr^{3+}
LDA	21937	21182	12794	12628
PBE0	20727	20229	14004	13804
BP	18028	17402	11979	11856
HF	26185	25817	19330	19086
experimental	25200[3]	24096[19]	15100[11]	15030[10]

[a]The corresponding experimental values are also reported. All transition energies are given in cm^{-1}.

In the same table the values of $E(^2E \rightarrow {}^4A_2)$ energies derived for Cr^{3+} in the two $KMgF_3$ and $LiBaF_3$ lattices using the four different approaches are also collected and compared to experimental findings. It can be noted that although the DFT values calculated for $KMgF_3$:Mn^{2+} and $LiBaF_3$:Mn^{2+} through the three functionals are somewhat smaller than the experimental ones, the results obtained are *consistent* with a relevant experimental observation,[3,19] namely the reduction of $E(^6A_1 \rightarrow {}^4A_1)$ when $KMgF_3$ is replaced by $LiBaF_3$ as host lattice. This trend is also reproduced in the HF calculation shown in Table 3.

If we call Δ the decrease of $E(^6A_1 \rightarrow {}^4A_1)$ when $KMgF_3$ is replaced by $LiBaF_3$, calculated Δ values using the three DFT functionals for the Mn^{2+} impurity (Table 3) are lying in the

dx.doi.org/10.1021/jp5010067 | J. Phys. Chem. A 2014, 118, 2377−2384

Table 4. Values (in cm^{-1}) of Exchange Integrals $K(x^2 - y^2, 3z^2 - r^2)$, $K(xy, 3z^2 - r^2)$, $K(xy, x^2 - y^2)$, and $K(xz, yz)$ Calculated for Mn^{2+}-Doped $KMgF_3$ and $LiBaF_3$ Lattices using the PBE0 and BP (in Parentheses) Functionals[a]

	$K(x^2 - y^2, 3z^2 - r^2)$	$K(xy, 3z^2 - r^2)$	$K(xy, x^2 - y^2)$	$K(xz, yz)$
$KMgF_3:Mn^{2+}$	5692 (4791)	5594 (4840)	2696 (2371)	4774 (4307)
$LiBaF_3:Mn^{2+}$	5612 (4622)	5469 (4670)	2623 (2291)	4661 (4202)
reduction (%)	1.4 (3.5)	2.2 (3.5)	2.7 (3.4)	2.4 (2.4)

[a]The relative reduction of the value of such integrals on passing from $KMgF_3:Mn^{2+}$ to $LiBaF_3:Mn^{2+}$ is also given.

Table 5. Values (in cm^{-1}) of Exchange Integrals $K(x^2 - y^2, 3z^2 - r^2)$, $K(xy, 3z^2 - r^2)$, $K(xy, x^2 - y^2)$, and $K(xz, yz)$ Calculated for Cr^{3+}-Doped $KMgF_3$ and $LiBaF_3$ Lattices using the PBE0 and BP (in Parentheses) Functionals[a]

	$K(x^2 - y^2, 3z^2 - r^2)$	$K(xy, 3z^2 - r^2)$	$K(xy, x^2 - y^2)$	$K(xy, xz)$
$KMgF_3:Cr^{3+}$	5112 (4121)	5093 (4275)	2563 (2242)	4668 (3993)
$LiBaF_3:Cr^{3+}$	5035 (3977)	4970 (4130)	2500 (2170)	4601 (3952)
reduction (%)	1.5 (3.5)	2.4 (3.4)	2.4 (3.2)	1.4 (1.0)

[a]The reduction of the value of such integrals on passing from $KMgF_3:Cr^{3+}$ to $LiBaF_3:Cr^{3+}$ is also given.

500−750 cm^{-1} range, while the experimental one is Δ = 1100 cm^{-1}. Furthermore, the present calculations give a relative reduction of $E(^2E \rightarrow {}^4A_2)$ for the Cr^{3+} impurity, which is smaller than that for $E(^6A_1 \rightarrow {}^4A_1)$. This fact is thus in reasonable agreement with experimental results.[3,10,11,19]

Values of exchange integrals $K(x^2 - y^2, 3z^2 - r^2)$, $K(xy, 3z^2 - r^2)$, $K(xy, x^2 - y^2)$, and $K(xz, yz)$ calculated for $KMgF_3$:M and $LiBaF_3$:M (M = Mn^{2+} and Cr^{3+}) at the corresponding equilibrium distance are displayed on Tables 4 and 5. For the sake of comparison, the results derived through both PBE0 and BP functionals are reported. It can be noted first of all that the value of exchange integrals decreases on passing from $KMgF_3$:M to $LiBaF_3$:M (M = Mn^{2+} and Cr^{3+}). Nevertheless, while under the substitution of $KMgF_3$ by $LiBaF_3$ as host lattice, $K(xy, 3z^2 - r^2)$ and $K(xy, x^2 - y^2)$ integrals are reduced by ∼3% for both impurities, the decrease of the $K(xz, yz)$ integral involving two π orbitals is smaller, especially for the Cr^{3+} impurity where the relative reduction is only around 1%. As $E(^2E \rightarrow {}^4A_2)$ is proportional to $K(xz, yz)$ (eq 2), while $E(^6A_1 \rightarrow {}^4A_1)$ depends on $K(xy, 3z^2 - r^2)$ and $K(xy, x^2 - y^2)$ (eq 6), the results gathered in Tables 4 and 5 are thus consistent with a higher sensitivity to the replacement of $KMgF_3$ by $LiBaF_3$ for the $^6A_1 \rightarrow {}^4A_1$ transition of Mn^{2+} than for the $^2E \rightarrow {}^4A_2$ sharp line of Cr^{3+}. At the same time, the results collected in Table 5 support that the quantity $\Delta(^4T_1; {}^4T_2)$, reflecting the energy difference of $^4A_2 \rightarrow {}^4T_1$ and $^4A_2 \rightarrow {}^4T_2$ transitions of Cr^{3+}, is more sensitive than $E(^2E \rightarrow {}^4A_2)$ to feel the substitution of $KMgF_3$ by $LiBaF_3$ as host lattice.[3,10,11,19,25] In fact, $\Delta(^4T_1; {}^4T_2)$ depends on Coulomb and exchange integrals involving one σ and one π electron.[26]

Despite the limitations of the present approach, restricted to configuration interactions within the d^n configuration (n = 3 for Cr^{3+} and n = 5 for Mn^{2+}), the calculated values of $E(^6A_1 \rightarrow {}^4A_1)$ and $E(^2E \rightarrow {}^4A_2)$ transition energies are not too far from the experimental quantities (Table 3) and shed light on the different behavior of sharp lines due to CrF_6^{3-} and MnF_6^{4-} complexes under the host lattice change. It is worth noting now that an overestimation of about 2500 cm^{-1} has been recently obtained for $E(^2E \rightarrow {}^4A_2)$ of $KMgF_3:Cr^{3+}$ by means of a calculation involving a configuration interaction well beyond the states emerging from the d^3 configuration.[26]

Let us see now whether the main trends shown in Tables 4 and 5 can be explained, considering only the changes in the charge of the central cation[30,40,41] taking place on passing from $KMgF_3$:M to $LiBaF_3$:M (M = Mn^{2+} and Cr^{3+}). To qualify this matter, let us now shortly write the wave function of antibonding orbitals like $t_{2g}(xy)$ or $e_g(x^2 - y^2)$ as follows

$$|t_{2g}(xy)\rangle = \eta_t|d_{xy}\rangle - \lambda_t|\chi_{xy}\rangle$$
$$|e_g(x^2 - y^2)\rangle = \eta_e|d_{x^2-y^2}\rangle - \lambda_e|\chi_{x^2-y^2}\rangle \quad (9)$$

where $|\chi_{xy}\rangle$ is a linear combination of ligand 2p(F) orbitals transforming like xy while in $|\chi_{x^2-y^2}\rangle$ there is also a hybridization between 2p(F) and 2s(F) orbitals, which is symmetry allowed. Several authors have *assumed*[26,30,41] that only the contribution to the exchange integrals coming from the two electrons residing on the central cation is important and then it can be written

$$K(xy, xz) = \eta_t^4 K^0(xz, yz)$$
$$K(xy, 3z^2 - r^2) = \eta_t^2\eta_e^2 K^0(xy, 3z^2 - r^2)$$
$$K(3z^2 - r^2, x^2 - y^2) = \eta_e^4 K^0(3z^2 - r^2, x^2 - y^2) \quad (10)$$

where in eq 10, the meaning of a quantity like $K^0(xy, x^2 - y^2)$ is simply described by

$$K^0(xy, x^2 - y^2) = \left\langle d_{xy}(1)d_{x^2-y^2}(2)\left|\frac{e^2}{r_{12}}\right|d_{xy}(2)\, d_{x^2-y^2}(1)\right\rangle \quad (11)$$

In an octahedral TM complex, the electronic charge on the metal for an antibonding σ orbital, q_e, is smaller than that for an antibonding π orbital, q_t, an idea well-verified in the present cases, as shown in Table 6. Thus, as q_e and q_t are certainly close to η_e^2 and η_t^2, respectively, we can expect that if eq 10 is right, the reduction undergone by $K(3z^2- r^2, x^2 - y^2)$ on passing from $KMgF_3$:M to $LiBaF_3$:M (M = Mn^{2+}, Cr^{3+}) will clearly be

Table 6. Values of η_e^2 and η_t^2 Parameters (in %) Calculated for Antibonding e_g ($\sim 3z^2 - r^2, x^2 - y^2$) and t_{2g} ($\sim xy, xz, yz$) Orbitals of $KMgF_3$:M and $LiBaF_3$:M (M = Mn^{2+} and Cr^{3+}) Using the BP Functional

	$KMgF_3:Cr^{3+}$	$LiBaF_3:Cr^{3+}$	$KMgF_3:Mn^{2+}$	$LiBaF_3:Mn^{2+}$
η_e^2	67.56	64.97	80.92	76.60
η_t^2	75.22	76.15	86.75	86.40

dx.doi.org/10.1021/jp5010067 | J. Phys. Chem. A 2014, 118, 2377−2384

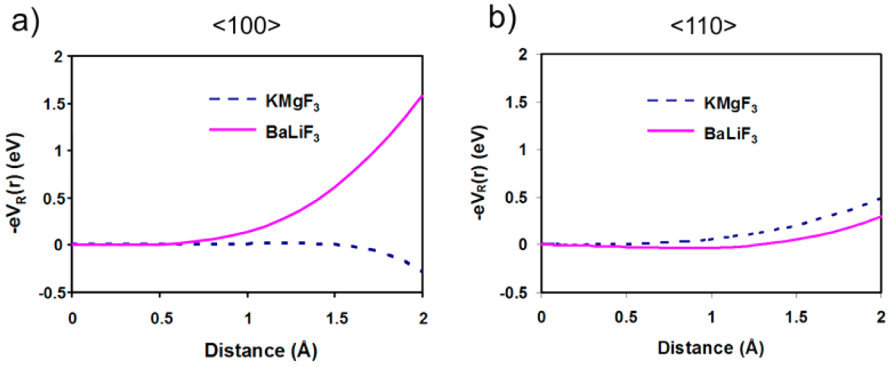

Figure 2. (a) Electrostatic potential, $V_R(\mathbf{r})$, of the rest of lattice ions on a MnF_6^{4-}/CrF_6^{3-}complex depicted along ⟨100⟩ type directions for $BaLiF_3$ (pink solid line) and $KMgF_3$ (blue dashed line). (b) The same for ⟨110⟩ type directions.

higher than that for $K(xy, 3z^2 - r^2)$. However, this conclusion is *not supported* by the results displayed in Tables 4 and 5, thus pointing out that the assumptions behind eq 10 are not correct. In the same vein, the higher variation of $K(xz, yz)$ for Mn^{2+} than for Cr^{3+} when $KMgF_3$ is replaced by $LiBaF_3$ can hardly be understood through the calculated η_t^2 values shown in Table 6.

It is worth noting now that there are two drastic assumptions behind the validity of eq 10. On the one hand, eq 10 assumes that if the two involved electrons are not on the metal, such a contribution to the exchange integrals can be neglected.[30,41] On the other hand, when the type of host lattice, and thus $V_R(\mathbf{r})$, is varied or simply the metal−ligand distance, R, of a given system is changed, the form of $|d_{xy}\rangle$ and $|d_{x^2-y^2}\rangle$ or $|\chi_{x^2-y^2}\rangle$ wave functions is *assumed* to remain *unmodified*. The last assumption has recently been verified to be incorrect[26] because the amount of sp hybridization in $|\chi_{x^2-y^2}\rangle$ is modified by changing $V_R(\mathbf{r})$ or the metal−ligand distance. Moreover, it is worth noting that $|d_{xy}\rangle$ and $|d_{x^2-y^2}\rangle$ wave functions are *not fixed* fragments as they are written as a combination of Slater or Gaussian orbitals where the involved coefficients are determined in the self-consistent procedure. For this reason, the shape of $|d_{xy}\rangle$ and $|d_{x^2-y^2}\rangle$ can also change when the internal electric field associated with $V_R(\mathbf{r})$ or the R distance is modified.

Let us now discuss the influence of the different shape of $V_R(\mathbf{r})$ potential in $KMgF_3$ and $LiBaF_3$ host lattices on the optical properties of Mn^{2+} and Cr^{3+} impurities. The form of $(-e)V_R(\mathbf{r})$ energy, when $\mathbf{r}$ is along the ⟨100⟩ and ⟨110⟩ directions for both host lattices is portrayed on Figure 2. The differences in $V_R(\mathbf{r})$ potential between $KMgF_3$ and $LiBaF_3$ lattices essentially come from the different nature of the first two shells of ions (Figure 1) lying outside the MF_6 complex (M = Mn^{2+} and Cr^{3+}).[25] So, while in $KMgF_3$, the first shell is made of monovalent cations and the second one involves divalent cations, the opposite happens in $LiBaF_3$. It can be remarked that when $\mathbf{r}$ is along a ⟨100⟩ direction $(-e)V_R(\mathbf{r})$ is practically constant in the normal perovskite, while in the inverted one it tends to increase the electron energy when we go from $\mathbf{r} = 0$ to the ligand region. Therefore, $(-e)V_R(\mathbf{r})$ induces an *extra increment* of the e_g level energy when $LiBaF_3$ is the host lattice, thus giving rise to a 10Dq value which is only ∼12% higher than for $KMgF_3$:M (M = Mn^{2+}, Cr^{3+}).[25,26] Moreover, the smallness of this relative shift of 10Dq due to $V_R(\mathbf{r})$ strongly suggests that it can basically be understood *just* considering *first-order* effects. In other words, if we designate by $|e_g^0(i)\rangle$ (i = $3z^2 - r^2$, $x^2 - y^2$) and $|t_{2g}^0(j)\rangle$ (j = xy, xz, yz), the frozen wave functions corresponding to the isolated CrF_6^{3-} and MnF_6^{4-} complexes, then the increase of 10Dq, $\delta(10Dq)$, induced by a nonconstant $V_R(\mathbf{r})$ potential on the complex, is essentially given by the first-order contribution

$$\delta(10Dq) \cong (-e)\{\langle e_g^0(i)|V_R(\mathbf{r})|e_g^0(i)\rangle - \langle t_{2g}^0(j)|V_R(\mathbf{r})|t_{2g}^0(j)\rangle\} \quad (12)$$

As the addition of $V_R(\mathbf{r})$ to isolated CrF_6^{3-} and MnF_6^{4-} complexes keeps the cubic symmetry, an antibonding orbital like e_g can only be mixed with orbitals of the same label. In these fluoride complexes, the closest level belonging to e_g is just the bonding e_g^b orbital mainly made from 2p(F) orbitals of six ligands. The energy difference between e_g and e_g^b orbitals, $\varepsilon(e_g) - \varepsilon(e_g^b)$, typically lies between 60000 and 90000 cm^{-1} for fluoride complexes.[42−46] Accordingly, if $\delta(10Dq) \approx 1.5 \times 10^3$ cm^{-1} is essentially the first-order correction to the energy of the e_g orbital due to $V_R(\mathbf{r})$, $\varepsilon_1(e_g)$, then the second-order correction, $\varepsilon_2(e_g)$, will be *of the order of* $[\delta(10Dq)]^2/[\varepsilon(e_g) - \varepsilon(e_g^b)]$ and thus smaller than 100 cm^{-1}. This rough argument underlines that the effects of $V_R(\mathbf{r})$ on antibonding orbitals of CrF_6^{3-} and MnF_6^{4-} complexes in cubic lattices can reasonably be understood through a perturbative approach. A wider discussion on this relevant matter has recently been reported.[47,48]

The present reasoning thus explains why the relative shift undergone by $E(^2E \rightarrow {}^4A_2)$ and $E(^6A_1 \rightarrow {}^4A_1)$ transition energies is much smaller than that corresponding to 10Dq. In fact, exchange integrals like $K(xy, 3z^2 - r^2)$ or $K(xz, yz)$ are unmodified if the electronic density is kept frozen, and thus variations in $E(^6A_1 \rightarrow {}^4A_1)$ and $E(^2E \rightarrow {}^4A_2)$ due to the addition of $V_R(\mathbf{r})$ appear *only in second-order* perturbations. This fact together with the small sensitivity of $K(xz, yz)$ to changes of $V_R(\mathbf{r})$ specially for Cr^{3+} are thus likely to be responsible for the tiny variations of $E(^2E \rightarrow {}^4A_2)$ (smaller than 2%) observed along the series of oxides containing CrO_6^{9-} complexes (Table 1).

Looking at Figure 2, it is clear that $(-e)V_R(\mathbf{r})$ for $LiBaF_3$ tends to move the total electronic charge from the ligand region toward the open shell central cation. Nevertheless, this shift does not happen for every orbital of the complex. Indeed, as an antibonding orbital like e_g has to be always orthogonal to the bonding counterpart, e_g^b, the shift of the electronic charge under the action of $V_R(\mathbf{r})$ is different for the filled e_g^b orbital and the partially filled e_g orbitals. So, the action of $(-e)V_R(\mathbf{r})$ increases the presence of electrons in the metal region for bonding levels, while the opposite happens for antibonding levels which spend more time in the ligand region. As bonding orbitals are fully populated but not the antibonding ones, this

dx.doi.org/10.1021/jp5010067 | J. Phys. Chem. A 2014, 118, 2377−2384

process gives rise to a *net flow* of electronic charge from ligands to the metal cation.[25] This explains, albeit qualitatively, that q_e is reduced when a practically constant $V_R(\mathbf{r})$, characteristic of a normal perovskite, is replaced by that corresponding to $LiBaF_3$.

5. FINAL REMARKS

Main conclusions of the present work are the following: (1) The effects of host lattice change on the properties of a MX_6 complex embedded in an insulating lattice can essentially be understood *just* considering the *complex but subject* to the electrostatic potential coming from the rest of lattice ions, $V_R(\mathbf{r})$. (2) When we properly describe the multiplets of 3d impurities under O_h symmetry within the $3d^n$ configuration, the different sensitivity of $E(^2E \rightarrow {}^4A_2)$ and $E(^6A_1 \rightarrow {}^4A_1)$ transition energies to host lattice changes can reasonably be understood. Indeed, the former depends on the exchange integral $K(yz, xz)$, where the two electrons have a π character, while $E(^6A_1 \rightarrow {}^4A_1)$ depends on $K(3z^2 - r^2, xy)$ and $K(x^2 - y^2, xy)$, reflecting the exchange between a π and another σ electron. This crucial difference is however *missed* in the usual Tanabe-Sugano approach. (3) The variations undergone by $K(xz, yz)$, $K(3z^2 - r^2, xy)$, $K(x^2 - y^2, xy)$ and $K(3z^2 - r^2, x^2 - y^2)$ exchange integrals under a host lattice substitution cannot be accounted for considering *only the changes of covalency* in a simple way. (4) As the action of $V_R(\mathbf{r})$ modifies the electronic density only in second-order perturbations, this explains why exchange integrals like $K(yz, xz)$ or $K(3z^2 - r^2, xy)$, and thus $E(^2E \rightarrow {}^4A_2)$ and $E(^6A_1 \rightarrow {}^4A_1)$, are much less sensitive to host lattice changes than transitions which do depend on 10Dq. (5) Bearing in mind that the exchange integral, $K(xz, yz)$ for Cr^{3+} complexes, is specially resistant to variations of the $V_R(\mathbf{r})$ potential due to the rest of the lattice ions, this allows one to understand why $E(^2E \rightarrow {}^4A_2)$ energy is constant within 2% for the series of oxides doped with such an impurity. (6) Although the usual Tanabe−Sugano approach involving only the two B and C parameters can be useful for assigning the optical bands observed experimentally, such approach is *not reliable* for understanding *finer details* such as those analyzed in the present work.

Despite the present calculations carried out on small clusters and restricted to the d^n configuration ($n = 3$ for Cr^{3+} and $n = 5$ for Mn^{2+}), they open a window for gaining better insight into the influence of an insulating lattice upon the optical transitions of a TM impurity. In particular, the results shown in this work stress the importance of the $V_R(\mathbf{r})$ potential for understanding the variations of optical properties of TM complexes placed in host lattices which are not *isomorphous*. Nevertheless, the role played by this internal electrostatic potential is often missed when reviewing the properties of an impurity in different host lattices.[49]

The present results underline the difficulties for a right understanding of crystal-field transitions of TM complexes embedded in insulating lattices when the symmetry is lower than cubic. Along this line, it has recently been pointed out that the $d_{x^2-y^2} - d_{3z^2-r^2}$ splitting observed for D_{4h} CuF_6^{4-} units in insulating fluorides is, in general, not directly related to the tetragonal distortion in the complex.[50]

It is worth noting now that EPR measurements carried out on $LiBaF_3:Cr^{3+}$ suggest[10] that most of the centers formed involve a Ba^{2+} vacancy and thus the symmetry around the CrF_6^{3-} unit is not perfectly cubic. Nevertheless, a detailed study performed on $MgO:Cr^{3+}$ proves that a close Mg^{2+} vacancy has practically no effect on the value of $E(^2E \rightarrow {}^4A_2)$. Indeed if $E(^2E \rightarrow {}^4A_2) = 14325\ cm^{-1}$ for the perfect octahedral CrO_6^{9-} unit in MgO, the corresponding value measured for the C_{4V} center involving a near Mg^{2+} vacancy[20] is practically identical being *only* 0.5% smaller.

Bearing the present analysis in mind, a similar procedure to that employed in this work can also be applied for exploring the effects of applied pressures upon the multiplets of TM complexes embedded in insulating lattices. Work along this line is now in progress.

AUTHOR INFORMATION

Corresponding Author

*E-mail: jumagala@fysik.dtu.dk.

Notes

The authors declare no competing financial interest.

ACKNOWLEDGMENTS

The support by the Spanish Ministry of Economy and Competitiveness under Projects FIS2012-30996 and FIS2009-07083 is acknowledged. J.M.G.L. also acknowledges support from the Spanish Ministry of Economy and Competitiveness under Project FIS2010-21282-C02-01.

REFERENCES

(1) Henderson, B.; Imbush, G. F. *Optical Spectroscopy of Inorganic Solids*; Oxford Science Publications: Oxford, 1989.

(2) Duclos, S. J.; Vohra, Y. K.; Ruoff, A. L. Pressure-Dependence of the $^4T_2$ and $^4T_1$ Absorption-Bands of Ruby to 35 GPa. *Phys. Rev. B* **1990**, *41* (8), 5372−5381.

(3) Rodriguez, F.; Moreno, M.; Tressaud, A.; Chaminade, J. P. Mn^{2+} in Cubic Perovskites: Determination of the Mn^{2+}-F^- Distance from the Optical-Spectrum. *Cryst. Lattice Defects Amorphous Mater.* **1987**, *16* (1−4), 221−225.

(4) Jacobsen, S. M.; Tissue, B. M.; Yen, W. M. New Methods for Studying the Optical-Properties of Metal-Ions in Solids. *J. Phys. Chem.* **1992**, *96* (4), 1547−1553.

(5) Trueba, A.; Garcia-Fernandez, P.; Garcia-Lastra, J. M.; Aramburu, J. A.; Barriuso, M. T.; Moreno, M. Spectrochemical Series and the Dependence of Racah and 10Dq Parameters on the Metal-Ligand Distance: Microscopic Origin. *J. Phys. Chem. A* **2011**, *115* (8), 1423−1432.

(6) Moreno, M.; Aramburu, J. A.; Barriuso, M. T. Electronic Properties and Bonding in Transition Metal Complexes: Influence of Pressure. *Optical Spectra and Chemical Bonding in Inorganic Compounds, Vol 1* **2004**, *106*, 127−152.

(7) Powell, R. C. *Physics of Solid State Laser Materials*; Springer: New York, 1998.

(8) Burns, R. G. *Mineralogical Applications of Crystal Field Theory*; Cambridge University Press: Cambridge, 1993.

(9) Wood, D. L.; Imbusch, G. F.; Macfarla, Rm; Kisliuk, P.; Larkin, D. M. Optical Spectrum of Cr3+ Ions in Spinels. *J. Chem. Phys.* **1968**, *48* (11), 5255.

(10) Mortier, M.; Gesland, J. Y.; Piriou, B.; Buzare, J. Y.; Rousseau, M. Spectroscopic Studies of Ni^{2+} or Cr^{3+}-Dped $BaLiF_3$. *Opt. Mater.* **1994**, *4* (1), 115−120.

(11) Mortier, M.; Wang, Q.; Buzare, J. Y.; Rousseau, M.; Piriou, B. Optical Studies of Cr^{3+} in $KMgF_3$: Time-Resolved Site-Selective Spectroscopy and Experimental Evidence of Spin-Orbit Coupling. *Phys. Rev. B* **1997**, *56* (6), 3022−3031.

(12) Freire, P. T. C.; Pilla, O.; Lemos, V. Pressure-Induced Level-Crossing in $KZnF_3:Cr^{3+}$. *Phys. Rev. B* **1994**, *49* (13), 9232−9235.

(13) Dolan, J. F.; Rinzler, A. G.; Kappers, L. A.; Bartram, R. H. Pressure and Temperature-Dependence of Chromium Photoluminescence Spectra in Fluoride Elpasolites. *J. Phys. Chem. Solids* **1992**, *53* (7), 905−912.

(14) Wein, G. R.; Hamilton, D. S.; Sliwczuk, U.; Rinzler, A. G.; Bartram, R. H. Two-Photon Excitation Spectroscopy of Cr^{3+}: K_2NaScF_6 Elpasolite: I. Experimental Aspects. *J. Phys.: Condens. Matter* **2001**, *13* (10), 2363−2375.
(15) Delucas, C. M.; Rodriguez, F.; Dance, J. M.; Moreno, M.; Tressaud, A. Luminescence of the New Elpasolite Rb_2KGaF_6 Doped with Cr^{3+}. *J. Lumin.* **1991**, *48*−*9*, 553−557.
(16) Tanner, P. A. Fluorescence and Phosphorescence of Cr^{3+} in Cubic Hosts. *Chem. Phys. Lett.* **2004**, *388* (4−6), 488−493.
(17) Pedro, S. S.; Sosman, L. P.; Barthem, R. B.; Tedesco, J. C. G.; Bordallo, H. N. Effects of Cr^{3+} Concentration on the Optical Properties of Cs_2NaAlF_6 Single Crystals. *J. Lumin.* **2013**, *134*, 100−106.
(18) Yosida, T. The ENDOR Investigations of $LiBaF_3$:Mn^{2+} Having the Inverse Perovskite Structure. *J. Phys. Soc. Jpn.* **1980**, *49* (1), 127−135.
(19) Henke, B.; Secu, M.; Rogulis, U.; Schweizer, S.; Spaeth, J. M. Optical and magneto-Optical Studies on Mn-Activated $LiBaF_3$. *Phys. Status Solidi C* **2005**, *2*, 380.
(20) Henry, M. O.; Larkin, J. P.; Imbusch, G. F. Nature of Broad-Band Luminescence Center in MgO:Cr^{3+}. *Phys. Rev. B* **1976**, *13* (5), 1893−1902.
(21) Duvarney, R. C.; Niklas, J. R.; Spaeth, J. M. ENDOR Study of Cubic Fe^{3+} Centers in $KMgF_3$. *Phys. Status Solidi B* **1981**, *103* (1), 329−336.
(22) Moreno, M.; Barriuso, M. T.; Aramburu, J. A.; Garcia-Fernandez, P.; Garcia-Lastra, J. M. Microscopic Insight into Properties and Electronic Instabilities of Impurities in Cubic and Lower Symmetry Insulators: The Influence of Pressure. *J. Phys.: Condens. Matter* **2006**, *18* (17), R315−R360.
(23) Garcia-Lastra, J. M.; Barriuso, M. T.; Aramburu, J. A.; Moreno, M. Origin of the Different Color of Ruby and Emerald. *Phys. Rev. B* **2005**, *72* (11), 113104.
(24) Garcia-Lastra, J. M.; Aramburu, J. A.; Barriuso, M. T.; Moreno, M. Optical Properties of Cr^{3+}-Doped Oxides: Different Behavior of Two Centers in Alexandrite. *Phys. Rev. B* **2006**, *74* (11), 115118.
(25) Trueba, A.; Garcia-Lastra, J. M.; Barriuso, M. T.; Aramburu, J. A.; Moreno, M. Influence of Internal Electric Fields on Bonding and Properties of Impurities in Insulators: Mn^{2+} in $LiBaF_3$ and Normal Perovskites. *Phys. Rev. B* **2008**, *78* (7), 075108.
(26) Trueba, A.; Garcia-Lastra, J. M.; Garcia-Fernandez, P.; Aramburu, J. A.; Barriuso, M. T.; Moreno, M. Cr^{3+}-Doped Fluorides and Oxides: Role of Internal Fields and Limitations of the Tanabe−Sugano Approach. *J. Phys. Chem. A* **2011**, *115* (46), 13399−13406.
(27) Sugano, S.; Tanabe, Y.; Kamimura, H. *Multiplets of Transition-Metal Ions in Crystals*; Academic Press: New York, 1970.
(28) Griffith, J. S. *The Theory of Transition-Metal Ions*; Cambridge University Press: Cambridge, 1961.
(29) Tofield, B. C. Covalency Effect in Magnetic Interactions. *Journal de Physique Colloques* **1976**, *37* (C6−539), C6−570.
(30) Curie, D.; Barthou, C.; Canny, B. Covalent Bonding of Mn^{2+} Ions In Octahedral and Tetrahedral Coordination. *J. Chem. Phys.* **1974**, *61* (8), 3048−3062.
(31) Stout, J. W. Absorption Spectrum of Manganous Fluoride. *J. Chem. Phys.* **1959**, *31* (3), 709−719.
(32) te Velde, G.; Bickelhaupt, F. M.; Baerends, E. J.; Guerra, C. F.; Van Gisbergen, S. J. A.; Snijders, J. G.; Ziegler, T. Chemistry with ADF. *J. Comput. Chem.* **2001**, *22* (9), 931−967.
(33) Vosko, S. H.; Wilk, L.; Nusair, M. Accurate Spin-Dependent Electron Liquid Correlation Energies for Local Spin-Density Calculations: A Critical Analysis. *Can. J. Phys.* **1980**, *58* (8), 1200−1211.
(34) Becke, A. D. Density-Functional Exchange-Energy Approximation with Correct Asymptotic-Behavior. *Phys. Rev. A* **1988**, *38* (6), 3098−3100.
(35) Perdew, J. P. Density-Functional Approximation for the Correlation-Energy of the Inhomogeneous Electron-Gas. *Phys. Rev. B* **1986**, *33* (12), 8822−8824.
(36) Adamo, C.; Barone, V. Toward Reliable Density Functional Methods Without Adjustable Parameters: The PBE0Model. *J. Chem. Phys.* **1999**, *110* (13), 6158−6170.
(37) Piken, A. G.; van Gool, W. Ford Motor Company Technical Report No. SL 68−10, 1968; Program modified by Aramburu, J. A., 1996.
(38) Atanasov, A.; Daul, C. A.; Rauzy, C.; Based, A. DFT Ligand Field Theory. In *Optical Spectra and Chemical Bonding in Inorganic Compounds, Vol 1*; Schoenherr, T., Ed.; Springer-Verlag: Berlin, 2004; Vol. *106*, pp 97−125.
(39) Atanasov, M.; Daul, C. A.; Rauzy, C. New Insights into the Effects of Covalency on the Ligand Field Parameters: A DFT Study. *Chem. Phys. Lett.* **2003**, *367* (5−6), 737−746.
(40) Barriuso, M. T.; Aramburu, J. A.; Moreno, M. Mn^{2+} Impurities in Fluoroperovskites: A Test for Theoretical Calculations. *J. Phys.: Condens. Matter* **1999**, *11* (48), L525−L530.
(41) Koide, S.; Pryce, M. H. L. Intensity Calculation of Some Optical Absorption Lines in Hydrated Manganous Salts. *Philos. Mag.* **1958**, *3* (30), 607−624.
(42) Simonetti, J.; McClure, D. S. Electron-Transfer Bands of the Divalent 3d Transition Series Ions in LiCl. *J. Chem. Phys.* **1979**, *71* (2), 793−801.
(43) Hirako, S.; Onaka, R. Charge-Transfer Bands of LiCl-M^{2+} and LiBr-M^{2+} (M = Mn, Fe, Co, Ni, and Cu). *J. Phys. Soc. Jpn.* **1982**, *51* (4), 1255−1263.
(44) Jörgensen, C. K. *Modern Aspects of Ligand Field Theory*; Nord Holland: Amsterdam, 1971.
(45) Aramburu, J. A.; Barriuso, M. T.; Moreno, M. An Insight into Charge-Transfer Transitions and their Bandwidths: Analysis of $Na_3In_2Li_3F_{12}$:Cr^{3+}. *J. Phys.: Condens. Matter* **1996**, *8* (37), 6901−6910.
(46) Pollini, I. Photoemission-Study of the Electronic-Structure of $CrCl_3$ and $RuCl_3$ Compounds. *Phys. Rev. B* **1994**, *50* (4), 2095−2103.
(47) Aramburu, J. A.; Garcia-Fernandez, P.; Garcia-Lastra, J. M.; Barriuso, M. T.; Moreno, M. Internal Electric Fields and Color Shift in Cr^{3+}-Based Gemstones. *Phys. Rev. B* **2012**, *85* (24), 245118.
(48) Aramburu, J. A.; Garcia-Fernandez, P.; Garcia-Lastra, J. M.; Barriuso, M. T.; Moreno, M. Colour due to Cr^{3+} Ions in Oxides: A Study of the Model System MgO:Cr^{3+}. *J. Phys.: Condens. Matter* **2013**, *25* (17), 175501.
(49) Wang, L.; Tan, L.; Hou, T.; Shi, J. Investigation of Change Regularity of Energy States of Mn^{2+} in Halides. *J. Lumin.* **2013**, *134*, 319−324.
(50) Garcia-Fernandez, P.; Barriuso, M. T.; Garcia-Lastra, J. M.; Moreno, M.; Aramburu, J. A. Compounds Containing Tetragonal Cu^{2+} Complexes: Is the $d_{x^2-y^2}$-$d_{3z^2-r^2}$ Gap a Direct Reflection of the Distortion? *J. Phys. Chem. Lett.* **2013**, *4* (14), 2385−2390.